Precision Medicine and Imaging

Clinical Cancer Research

Acquired Resistance Mutations to ALK Inhibitors Identified by Single Circulating Tumor Cell Sequencing in *ALK*-Rearranged Non–Small-Cell Lung Cancer

Emma Pailler[1,2,3], Vincent Faugeroux[1,2,3], Marianne Oulhen[1,2], Laura Mezquita[4], Mélanie Laporte[5], Aurélie Honoré[5], Yann Lecluse[6], Pauline Queffelec[1,2], Maud NgoCamus[4], Claudio Nicotra[4], Jordi Remon[4], Ludovic Lacroix[5], David Planchard[4], Luc Friboulet[2,3], Benjamin Besse[3,4], and Françoise Farace[1,2,3]

Abstract

Purpose: Patients with anaplastic lymphoma kinase (*ALK*)–rearranged non–small-cell lung cancer (NSCLC) inevitably develop resistance to ALK inhibitors. New diagnostic strategies are needed to assess resistance mechanisms and provide patients with the most effective therapy. We asked whether single circulating tumor cell (CTC) sequencing can inform on resistance mutations to ALK inhibitors and underlying tumor heterogeneity in *ALK*-rearranged NSCLC.

Experimental Design: Resistance mutations were investigated in CTCs isolated at the single-cell level from patients at disease progression on crizotinib ($n = 14$) or lorlatinib ($n = 3$). Three strategies including filter laser-capture microdissection, fluorescence activated cell sorting, and the DEPArray were used. One hundred twenty-six CTC pools and 56 single CTCs were isolated and sequenced. Hotspot regions over 48 cancer-related genes and 14 ALK mutations were examined to identify *ALK*-independent and *ALK*-dependent resistance mechanisms.

Results: Multiple mutations in various genes in ALK-independent pathways were predominantly identified in CTCs of crizotinib-resistant patients. The RTK-KRAS (*EGFR, KRAS, BRAF* genes) and TP53 pathways were recurrently mutated. In one lorlatinib-resistant patient, two single CTCs out of 12 harbored *ALK* compound mutations. CTC-1 harbored the $ALK^{G1202R/F1174C}$ compound mutation virtually similar to $ALK^{G1202R/F1174L}$ present in the corresponding tumor biopsy. CTC-10 harbored a second $ALK^{G1202R/T1151M}$ compound mutation not detected in the tumor biopsy. By copy-number analysis, CTC-1 and the tumor biopsy had similar profiles, whereas CTC-10 harbored multiple copy-number alterations and whole-genome duplication.

Conclusions: Our results highlight the genetic heterogeneity and clinical utility of CTCs to identify therapeutic resistance mutations in *ALK*-rearranged patients. Single CTC sequencing may be a unique tool to assess heterogeneous resistance mechanisms and help clinicians for treatment personalization and resistance options to ALK-targeted therapies.

Introduction

Selective anaplastic lymphoma kinase (ALK) tyrosine kinase inhibitors (TKIs) have dramatically transformed the therapeutic landscape for patients with *ALK*-rearranged non–small-cell lung cancer (NSCLC). The first FDA-approved ALK inhibitor was crizotinib which produced in randomized phase III trials significant improvements in objective response rates and progression-free survival (PFS) compared with chemotherapy, but most patients relapsed within the first year of treatment (1–3). Second-generation ALK inhibitors including ceritinib, alectinib, or brigatinib have been approved for patients who progressed on crizotinib, although resistance almost always develops (4–7). Due to their ability to improve PFS and control brain metastases, these drugs are also

[1]Gustave Roussy, Université Paris-Saclay, "Rare Circulating Cells" Translational Platform, CNRS UMS3655 – INSERM US23 AMMICA, Villejuif, France. [2]INSERM, U981 "Identification of Molecular Predictors and New Targets for Cancer Treatment," Villejuif, France. [3]Univ Paris Sud, Université Paris-Saclay, Faculty of Medicine, Le Kremlin-Bicêtre, France. [4]Gustave Roussy, Université Paris-Saclay, Department of Medicine, Villejuif, France. [5]Gustave Roussy, Université Paris-Saclay, Genomic Platform and Biobank, Department of Medical Biology and Pathology, CNRS UMS3655 – INSERM US23 AMMICA, Villejuif, France. [6]Gustave Roussy, Université Paris-Saclay, "Flow Cytometry and Imaging" Platform, CNRS UMS3655 – INSERM US23 AMMICA, Villejuif, France.

Note: Supplementary data for this article are available at Clinical Cancer Research Online (http://clincancerres.aacrjournals.org/).

B. Besse and F. Farace contributed equally to this article.

Current address for E. Pailler: Department of Medical Oncology, Dana-Farber Cancer Institute/Harvard Medical School/Broad Institute of Harvard and MIT, Boston, MA 02215.

Corresponding Author: Françoise Farace, Gustave Roussy, Université Paris-Saclay, "Rare Circulating Cells" Translational Platform, CNRS UMS3655 – INSERM US23 AMMICA, F-94805 Villejuif, France. Phone: 33142115198; E-mail: francoise.farace@gustaveroussy.fr

Clin Cancer Res 2019;25:6671–82

doi: 10.1158/1078-0432.CCR-19-1176

Translational Relevance

The standard-of-care treatment for anaplastic lymphoma kinase (*ALK*)–rearranged non–small-cell lung cancer is based on selective ALK inhibitors, but drug resistance almost always develops leading to clinical relapse. Resistance to ALK inhibitors can be fostered by multiple different molecular mechanisms, identification of which is critical to provide the most effective therapy. As repeated tumor biopsies are not always feasible and representative of tumor heterogeneity, noninvasive alternative strategies are crucial to develop. Circulating tumor cells (CTCs) are likely released from spatially distinct metastatic sites and may provide a comprehensive genomic picture of the heterogeneity of resistance mechanisms to ALK inhibitors. Here, we show that sequencing CTCs at disease progression on crizotinib or lorlatinib can reveal highly heterogeneous mutational profiles in both ALK-independent and ALK-dependent pathways that cannot be detected in the corresponding tumor biopsy. Our results indicate that single CTC sequencing may be a unique tool to identify therapeutic resistance mechanisms. This can help clinicians to personalize ALK-targeted therapies which may ultimately translate into improved patient outcomes.

frequently prescribed upfront. Third-generation ALK inhibitors including lorlatinib and ensartinib are currently investigated (8, 9). Lorlatinib demonstrated clinical activity in resistant patients previously treated with two or more ALK inhibitors including second-generation inhibitors (10). Multiple different resistance mechanisms to ALK inhibitors were identified in postprogression tumor specimens including either "on-target" genetic alterations or "off-target" mechanisms, which may involve activation of parallel/downstream pathways or lineage transdifferentiation (6, 11). In published series, "on-target" resistance mechanism to crizotinib was mediated by somatic mutations distributed throughout the ALK kinase domain or gene copy-number gains in approximately one third of patients (12–15). In the majority of crizotinib-resistant patients, resistance occurred through the activation of other tyrosine kinase receptors such as EGFR, KRAS, or c-KIT, or an unidentified mechanism (12, 16). In some cases, multiple resistance mechanisms to crizotinib were observed in the same patient as well as the emergence of an *ALK* gene fusion–negative tumor (12, 16). In approximately half of cases, resistance to second-generation ALK inhibitors is caused by emergence of additional *ALK* mutations, the most common being the solvent-front substitution ALK^{G1202R} (13–15). Broad gene testing by comprehensive next-generation sequencing (NGS) revealed a high rate (~40%) of alterations in multiple bypass activating pathways including gene fusions (such as *RET*), copy-number variations, and somatic mutations in patients resistant to multiple lines of ALK-TKIs, which can be concomitant to the activation of ALK via *ALK* mutations (14, 15). Using mutagenesis screening and *in vivo* mouse models, resistance to lorlatinib was found to be mediated by compound *ALK* mutations (i.e., mutations located on the same allele; refs. 17, 18). The analysis of repeated tumor biopsies from lorlatinib-resistant patients indicated that compound *ALK* mutations were developed in a stepwise fashion in patients treated with sequential ALK inhibitors (17, 18). Because of the heterogeneity, complexity, and dynamic nature of resistance, improved outcomes for *ALK*-rearranged patients necessitate to personalize treatments based upon the monitoring of tumor mutational profiles and the identification of specific ALK resistance mechanism (19).

By fostering tumor adaptation and therapeutic failure, tumor heterogeneity represents a major challenge to personalized medicine. Single-site tumor biopsies may not capture the full spectrum of genetic alterations and heterogeneous resistance profiles present within a tumor and metastases (20, 21). In addition, repeated tumor biopsies to identify secondary resistance mutations are invasive and in certain cases not feasible. New tools are needed to better evaluate tumor heterogeneity and monitor tumor mutational profiles over time and throughout disease evolution. The liquid biopsy has emerged as a noninvasive and easily accessible alternative to tumor biopsies to assess tumor mutational status and monitoring genetic changes in "real-time" (22, 23). Among the liquid biopsy components, the circulating tumor DNA (ctDNA) is mainly passively released from apoptotic or necrotic tumor cells and has rapidly emerged in the last years as a useful and sensitive tool to monitor genetic alterations predictive of tumor relapse or minimal residual disease occurrence in posttreatment setting (24). Longitudinal ctDNA genotyping was recently reported to be an effective tool for detecting *ALK* mutations and tracking resistance mechanisms in patients progressing on ALK-TKIs (25, 26). In contrast to ctDNA, circulating tumor cells (CTC) are either apoptotic or alive, but viable CTCs contain tumorigenic cell clones with high relevance for metastatic progression (27). They are likely released from spatially distinct metastatic sites and may provide a more comprehensive genomic picture of tumor content than a single-site tumor biopsy (28). Importantly, CTCs can be analyzed at the single-cell level and exploited to manage the considerable challenge of tumor genetic heterogeneity and therapeutic resistance.

Using various CTC technologies, our and other groups have evaluated the clinical interest of CTCs for predictive molecular biomarker detection and genomic characterization in NSCLC (28–30). We previously developed filter-adapted FISH (FA-FISH) on ISET (isolation by size of epithelial tumor cells) microfilters and reported for the first time the possibility of detecting *ALK* and *ROS1* rearrangements in CTCs from NSCLC-positive patients (29–31). More recently we monitored CTC subsets with distinct *ALK*-FISH patterns on crizotinib treatment and reported a significant association between levels of CTCs with *ALK* copy-number aberration (CNA) and PFS (32). Because of the technical challenges imposed by the rarity and biological heterogeneity of CTCs, there are to our knowledge, very few studies that exploited single CTC analysis to investigate therapeutic resistance mechanisms and underlying tumor genetic heterogeneity in patients treated with TKI (33). Herein, we used three different technologies for individual CTC isolation and a rigorous sequencing workflow to investigate resistance mutations in CTCs from 17 crizotinib- or lorlatinib-resistant *ALK*-rearranged patients. We showed that sequencing CTCs at the single-cell level enabled to identify both "on-target" and "off-target" resistance mutations to these ALK-TKIs. This exploratory study provides new insights into the therapeutic resistance landscape and underlying tumor heterogeneity in *ALK*-rearranged patients.

Materials and Methods

Patients

The study (IDRCB2008-A00585-50) was conducted at Gustave Roussy in accordance with the Declaration of Helsinki. It was authorized by the French national regulation agency *Agence Nationale de Sécurité du Medicament et des produits de santé* and approved by the Ethics Committee and our Institutional Review Board. Informed-written consent was obtained from all patients. From March 2011 to May 2017, stage IV *ALK*-rearranged NSCLC patients were recruited into the study. We present here the results obtained in the first 17 patients analyzed at resistance to an ALK inhibitor. *ALK* rearrangement was tested in tumor by FISH, immunochemistry, or reverse transcription-PCR. Peripheral blood samples were collected into EDTA and Cell Save tubes at progression disease (PD). Medical records were reviewed, and clinical characteristics were collected retrospectively.

Description of the strategies for CTC enrichment, detection, and isolation

ISET-filtration, immunofluorescent staining, scanning, and isolation of ISET-enriched CTCs by laser microdissection. CTC enrichment by the ISET-filtration system (RareCells) was carried out as previously reported (31, 34, 35). The sensitivity of ISET-filtration was previously reported by Vona and colleagues (35). ISET-filters are composed of 10 spots, and each spot (filtration of 1 mL of blood per spot) was cut out individually for independent analysis. Individual spots were immobilized on glass slides using adhesive ribbon. Before immunofluorescence staining, a "snick" was made on each spot to allow precise relocation of cells on the laser microdissector LMD6500 (Leica Biosystems Richmond). Spots were rehydrated 5 minutes in TBS 1X (Thermo Fisher Scientific) at room temperature, and cell permeabilization was performed in TBS 1X-Triton X-100 0.2% (Roche, Sigma-Aldrich) for 7 minutes at room temperature. After washing with TBS 1X, cells were incubated 25 minutes in a humidity dark chamber with antibodies against epithelial, mesenchymal, and leukocyte markers. Epithelial markers included a mouse anti-pancytokeratins (CK) monoclonal antibody (clone A45-B/B3, AS Diagnostik) and a mouse anti-CK 7 (Dako) conjugated to Alexa Fluor (AF) 488 using the Zenon Mouse IgG Labeling Kit (Thermo Fisher Scientific) and a mouse anti-EpCAM/CD326 AF488 (clone VU1D9, Novus Biological) monoclonal antibody. An anti–N-cadherin AF546 (clone 32/NCadherin, BD Biosciences) was used as mesenchymal marker, and an anti-CD45 APC (clone HI30, BD Biosciences) was used as leukocyte marker. After two washes with TBS 1X-Tween20 0.05% (Dako) and one wash with TBS 1X, Hoechst 33342 (Sigma-Aldrich) was added and incubated for 10 minutes at room temperature. After two washes with TBS 1X-Tween20 0.05% and one wash with TBS 1X, ISET-spots were mounted between a slide and coverslip using Ibidi mounting medium (Biovalley) and immediately scanned with the ARIOL scanner (Leica Biosystems Richmond). Candidate CTCs were classified according to epithelial and mesenchymal marker expression and/or morphologic characteristics as previously described (31). A software called ALTER (Leica Biosystems Richmond) was developed in collaboration with Leica Biosystems to precisely transfer the coordinates of CTC positions on filters to the laser microdissector LMD6500. Slides were washed successively in TBS 1X-Tween20 0.05% and in TBS 1X to remove the coverslip and mounting medium. Then, slides were dried at 45°C for 5 minutes before being ionized so as to avoid static electricity during microdissection. After relocation using the 20X magnification, individual CTCs were microdissected from ISET-filters using the UV laser and collected in the cap of Opticaps 0.2 PCR tubes (Leica Biosystems Richmond). Individually microdissected CTCs were either grouped per pool of three to five CTCs or collected as single cells. Tubes were frozen at −80°C for at least 30 minutes.

Enrichment and detection of CTCs by the CellSearch and isolation of CTC-enriched using the DEPArray system. CTC enrichment using the CellSearch system (Menarini Silicon Biosystems) was performed using the CTC Kit on 7.5 mL of blood collected in CellSave tubes as previously described (34, 36). At the end of the run, the cartridge was immediately removed from the MagNest device to prevent cells from sticking to the cartridge surface and stored at 4°C in the dark. CTCs were identified as $DAPI^+/CK^+/CD45^-$ cells and enumerated according to the manufacturer's guidelines. Cells were removed from the CellSearch cartridge, and CTCs were isolated using the DEPArray system (Menarini Silicon Biosystems) according the manufacturer's protocol (37).

Enrichment of CTCs by RosetteSep, immunofluorescent staining, and isolation of CTCs by fluorescence-activated cell sorting. Negative selection of CTCs by the RosetteSep Human CD45 Depletion Cocktail (StemCell Technologies; https://www.stemcell.com/technical-resources/product-information/product-information-sheet.html) was performed according to the manufacturer's protocol starting from blood samples collected in CellSave tubes. Cells collected were washed with PBS 1X and centrifuged 5 minutes at 1,600 rpm. The cell pellet was suspended with 100 μL of fixative solution medium A from the Fix&Perm Kit (Thermo Fisher Scientific) and washed with PBS 1X. Cells were centrifuged 5 minutes at 1,300 rpm. The cell pellet was resuspended with 100 μL of permeabilization solution medium B from the Fix &Perm Kit and a rabbit anti-ALK (clone D5F3, Cell Signaling Technology) monoclonal antibody and incubated 20 minutes in the dark at room temperature. After a PBS 1x wash and a centrifugation, a secondary goat anti-rabbit AF488 antibody and 50 μL of staining reagent containing cytokeratins-PE (cytokeratins 8, 18, 19) and CD45-APC antibodies from the CellSearch reagent kit were added. The cell suspension was incubated 20 minutes in the dark at room temperature and then centrifuged. The cell pellet was resuspended in 300 μL of PBS 1X and kept at +4°C. Hoechst 33342 was added before cell sorting. Individual CTC isolation was performed using a BD FACSARIA III cell sorter (BD Biosciences) equipped with four lasers (a 405-nm laser, a 488-nm laser, a 561-nm laser, and a 640-nm laser). The system was run with 20 psi pressure, a 100-μm nozzle, and the yield precision mode. Cell sorting started by gating Hoechst positive elements. The second gate enabled selecting CD45-APC–negative events. Three populations including $DAPI^+/CD45\text{-}APC^-/CK\text{-}PE^+/ALK\text{-}AF488^-$, $DAPI^+/CD45\text{-}APC^-/CK\text{-}PE^-/ALK\text{-}AF488^+$, and $DAPI^+/CD45\text{-}APC^-/CK\text{-}PE^+/ALK\text{-}AF488^+$ cells were sorted and recovered in 96-well plate. As a control, 200 $DAPI^+/CD45\text{-}APC^+/CK\text{-}PE^-/ALK\text{-}AF488^-$ cells were sorted in a well. Plates were centrifuged 10 minutes at 1,200 rpm and frozen at −20°C for at least 30 minutes.

Cell lines

The description of the cell lines is provided in the Supplementary Method section.

Whole-genome amplification, quality controls, and dsDNA conversion

Whole-genome amplification (WGA) was performed using the Ampli1 WGA Kit (Menarini Silicon Biosystems) according to the manufacturer's instructions. Quality of Ampli1 WGA products was checked as previously reported (38). To increase the total dsDNA content in Ampli1 WGA products, ssDNA molecules were converted into dsDNA molecules using the Ampli1 ReAmp/ds Kit (Menarini Silicon Biosystems).

Isolation of genomic DNA from blood and tumor biopsies

Isolation of DNA from formalin-fixed paraffin-embedded tumor biopsies and whole-blood is described in the Supplementary Method section.

Library preparation and Ion Torrent–targeted NGS

Ampli1 WGA products were cleaned up with 1.8X SPRIselect Beads (Beckman Coulter) and then quantified using Qubit fluorometer (Life Technologies) according to the manufacturer's instructions. To analyze cancer-gene sequence variants, two targeted panels were used: the Ampli1 Cancer Hotspot Panel Custom Beta adapted from Ion Ampliseq CHP v2 by Menarini Silicon Biosystems covering 2,265 COSMIC hotspots regions across 315 amplicons of 48 cancer-related genes commonly mutated in cancer and an in-house panel targeted the tyrosine kinase domain in *ALK* and *EGFR* genes. The primers for the in-house panel were designed using the Ion AmpliSeq Designer with the assistance of the White-Glove Ion Torrent Team from Thermo Fisher (Life Technologies). According to recommendations of the Ion AmpliSeq library kit 2.0 protocol, 10 ng of each sample (CTCs, $DAPI^+/CD45^+$ cells, germline control DNA, biopsy) were amplified with the Ion AmpliseqHifi Master Mix. Primers used for amplification were partially digested by FuPa enzyme. The Ion Xpress Barcode adapters were added to amplicons during the ligation step to allow for subsequent pooling of the samples according to the manufacturer's instructions. Each individual library was quantified using the Qubit fluorometer. An equal amount of each library was pooled. Library pool was used for emulsion PCR amplification, and template-positive Ion Sphere Particles were enriched using the Ion OneTouch 2 Instrument or the Ion OneTouch ES Instrument or the Ion Chef System (Life Technologies). Sequencing was performed using appropriate Ion chips for the Ion Personal Genome Machine or the Ion S5 System (500 flows).

Library preparation and low-pass whole-genome sequencing

Ampli1 LowPass kit for Illumina (Menarini Silicon Biosystems) was used for preparing low-pass whole-genome sequencing (WGS) libraries from single cells. For high-throughput processing, the manufacturer's procedure was implemented in a fully automated workflow on a STARlet Liquid Handling Robot (Hamilton). Ampli1 LowPass libraries were normalized and sequenced by HiSeq 2500 instrument using 150 SR rapid-run mode.

Bioinformatic workflow for targeted NGS analysis

For targeted NGS analysis, the workflow of the bioinformatics analysis was established with the GeCo-advanced genomic consulting service from Integragen.

Sequence alignment and variant calling. Base calling was performed using the Real-Time Analysis software sequence pipeline (2.7.7) from Illumina with default parameters. Sequence reads from amplified DNA (CTCs and $DAPI^+/CD45^+$ cells) were trimmed for Ampli1 adapters with Cutadapt (1.14) (39). Reads were then aligned to the human genome build hg38/GRCh38.p7 using the Burrows–Wheeler Aligner (BWA) tool (40). Duplicated reads were removed using Sambamba (41). Variant calling of single-nucleotide variants (SNV) and small insertions/deletions was performed using the Broad Institute's GATK Haplotype Caller GVCF tool (3.7) for germline variants and MuTect2 tool (2.0, –max_alt_alleles_in_normal_count = 2; –max_alt_allele_in_normal_fraction = 0.04; –maxReadsInRegionPerSample = 100000) for somatic variants (42–44). Ensembl's Variant Effect Predictor (VEP, release 87) was used to annotate variants with respect to functional consequences (type of mutation and prediction of the functional impact on the protein by SIFT.2.2 and PolyPhen 2.2.2) and frequencies in public (dbSNP147, 1000 Genomes phase 3, ExAC r3.0, COSMIC v79) and in-house databases (45). To rescue variants not detected by Mutect2, we performed a simple base counting using bam-readcount (https://github.com/genome/bam-readcount; parameters -q 20 -b 20). We selected variants with a sequencing depth $\geq$50, $\geq$10 mutated reads, and a variant allele fraction (VAF) >3% if sample is a pool of CTCs or >10% if sample is a single CTC, and we removed variants detected in matched germline DNA or in $\geq$2 unrelated germline DNAs.

Allele drop-out and identification of somatic mutations. CTC and $DAPI^+/CD45^+$ cell (negative controls) DNA were amplified before sequencing. To estimate allele drop-out (ADO), we selected all reliable variants (single-nucleotide polymorphisms [SNPs]) in germline control or $DAPI^+/CD45^+$ cell DNA using HaplotypeCaller with the following post-filtering: coverage $\geq$50 in both samples, $\geq$5% of variant reads. We then compared the proportions of normal/variant reads in the germline control and $DAPI^+/CD45^+$ cell DNA using the Fisher exact test. Variants with a significant difference ($P < 0.05$), a VAF between 0.2 and 0.8 in germline control DNA, and <0.1 or >0.9 in the $DAPI^+/CD45^+$ cell DNA were considered to have undergone allele drop-out.

To determine the number of somatic variants in each CTC, the post-filtering steps were applied:

- SNV variants only
- VEP (https://uswest.ensembl.org/info/genome/variation/prediction/predicted_data.html) impact classification as high or moderate
- VAF in the normal (VAF_N) ≤ 0.01
- VAF in the tumor (VAF_T) ≥ 0.03 for pools of CTCs and 0.1 for unique CTC samples
- an in-house somatic score $\geq$3. This score is calculated as follows: somatic_score = $((VAF_T \times VAC_T)/(1 + VAC_N))^*10$ with VAC_T and VAC_N the variant allele counts in the tumor and normal samples, respectively
- in hotspot regions
- depth in normal and tumor samples $\geq$ 50
- present in less than six other CTC samples

Bioinformatic workflow for low-pass WGS

For the low-pass WGS, the workflow of the bioinformatics analysis was done by Menarini Silicon Biosystems.

Sequence alignment. The obtained FASTQ files were aligned to the hg19 human reference sequence using BWA version 0.7.12 (46).

CNA calling and ploidy determination. CNAs in the data were identified using Control-FREEC software (version 11.0; ref. 47). Ploidy level was automatically estimated by Menarini Silicon Biosystems pipeline for each library based on best fitting of profiles to underlying copy-number levels (37).

Results

Clinical characteristics

Between 2011 and 2017, 17 *ALK*-rearranged patients had blood sampling for CTC analysis following radiological PD on ALK-TKI. Baseline patients' clinical characteristics are summarized in Table 1. A majority of patients were nonsmokers or smokers <15 pack-years (88%). All tumors were adenocarcinoma. Fourteen patients experienced PD on first-line treatment with crizotinib, and three previously treated patients progressed on lorlatinib as second-line or beyond. The median treatment duration on crizotinib and lorlatinib was 10.4 months [95% confidence interval (CI), 4.7–20.9] and 13.6 months (95% CI, 4.2–19.1), respectively (Supplementary Table S1). Eight patients of the crizotinib cohort were reported previously (Supplementary Table S2; refs. 29, 32). Four patients underwent a postprogression tumor biopsy (detailed patient characteristics in Supplementary Table S2). Blood samples were performed on treatment or within 1 week of treatment discontinuation.

Individual CTC isolation and sequencing analysis

Based on our and other studies showing the superiority of ISET-filtration for high CTC recovery, we initially developed a CTC isolation strategy based on ISET enrichment prior to a multistep process including immunofluorescent staining for CTC identification (Supplementary Fig. S1A; refs. 28, 34, 48). Individual CTCs were isolated by laser microdissection (LMD) from ISET-filters and were either analyzed as true single cells or grouped in pools of three to five CTCs of similar phenotype prior to the molecular analysis. Given the fragility of CTCs and risk of DNA degradation during this whole experimental process, we initially analyzed pools of individual CTCs rather than true single CTCs. Because LMD is labor-intensive, time-consuming, and poorly adapted to the evaluation of clinical specimens, two other strategies were established in parallel. The second strategy involved hematopoietic blood-cell depletion, immunofluorescent staining, and individual CTC sorting by fluorescence-activated cell sorting (FACS; Supplementary Fig. S1B). In the third strategy, CTCs were enumerated by the CellSearch and individually isolated using the DEPArray system when they were in sufficient numbers (Supplementary Fig. S1C). According to these three strategies, 126 CTC pools and clusters, and 56 single-CTCs were isolated (Supplementary Table S2).

A molecular workflow was established including WGA using the ligation-mediated PCR based Kit (Ampli1 WGA kit, Menarini Silicon Biosystems) and qualification of CTC samples and matched negative controls ($DAPI^+/CD45^+$ cells) followed by targeted NGS using two panels (Supplementary Fig. S2; Supplementary Table S3). To investigate "off-target" resistance mutations, we used a first panel covering COSMIC hotspots regions of 48 cancer-related genes commonly mutated in cancer (Supplementary Fig. S2A; Supplementary Table S3). "On-target" resistance mutations were assessed by a second in-house NSCLC-specific panel targeting 14 *ALK* resistance mutations in the tyrosine kinase domain of ALK (Supplementary Fig. S2B; Supplementary Table S3). Quality controls of WGA and targeted NGS are shown in Supplementary Fig. S3. Among the 15 patients for whom the ADO percentage was assessable, variants undergone ADO were found for seven patients (median of 0%; range, 0%–45%). Depth of sequencing was superior to 50X in 95% of CTC samples. For the CTC samples, the median of amplicons with a coverage superior to 50X was 80% (range, 7%–95%). Over all CTC samples from the 17 patients, the uniformity of amplicon coverage was 56% (range, 6%–82%). The whole molecular process was validated by testing pools and single cells from an *EGFR*-mutant cell line (NCI-H1975) harboring known mutations (Supplementary Table S4).

Table 1. Demographics and clinical parameters

	Patients	
Clinical parameters	**Crizotinib resistance (*N* = 14)**	**Lorlatinib resistance (*N* = 3)**
Age at baseline y/o	54 (29–70)	42 (42–59)
Sex (%)		
Female	8 (57)	1 (33)
Male	6 (43)	2 (66)
Smoking status (%)		
Nonsmoker	7 (50)	3 (100)
Smoker <15 PY	5 (36)	0 (0)
Smoker ≥15 PY	2 (14)	0 (0)
Number of previous treatment lines (%)		
0	4 (29)	0 (0)
1	4 (29)	0 (0)
≥2	6 (42)	3 (100)
Number of previous treatment lines with prior ALK inhibitor (%)		
0	14 (100)	0 (0)
1	0 (0)	1 (34)
2	0 (0)	1 (33)
3	0 (0)	1 (33)
ECOG PS at baseline (%)		
0–1	13 (93)	2 (66)
≥2	1 (7)	1 (33)
Number of metastatic sites (%)		
1	4 (29)	0 (0)
≥2	10 (71)	3 (100)

Abbreviations: ECOG, Eastern Cooperative Oncology Group; PS, performance status; PY, pack-year; y/o, years old.

Detection of mutations in CTCs from crizotinib-resistant patients

We investigated the VAF of resistance mutations in CTCs from 14 *ALK*-rearranged patients progressing on crizotinib. All patients developed acquired resistance to crizotinib with the exception of P4 who developed primary resistance after 2 months of treatment. As published by our and other groups, *ALK*-rearranged patients may harbor variable numbers of CTCs with *ALK*-CNA (29, 32, 49). We reasoned that one single mutated CTC inside a pool of five CTCs harboring a gain of *ALK* copies may produce low VAF. We therefore set the VAF threshold at 3% for pools of CTCs and at 10% for single-CTC. Mutations were identified in CTC samples from nine of the 14 patients (Fig. 1; Supplementary Fig. S4). P4 harbored a $TP53^{R175H}$ mutation (VAF, 100%) in CTC-3 specimen which was also detected in the corresponding tumor biopsy (VAF, 53%). Two additional mutations in *PI3KCA* and *TP53* genes

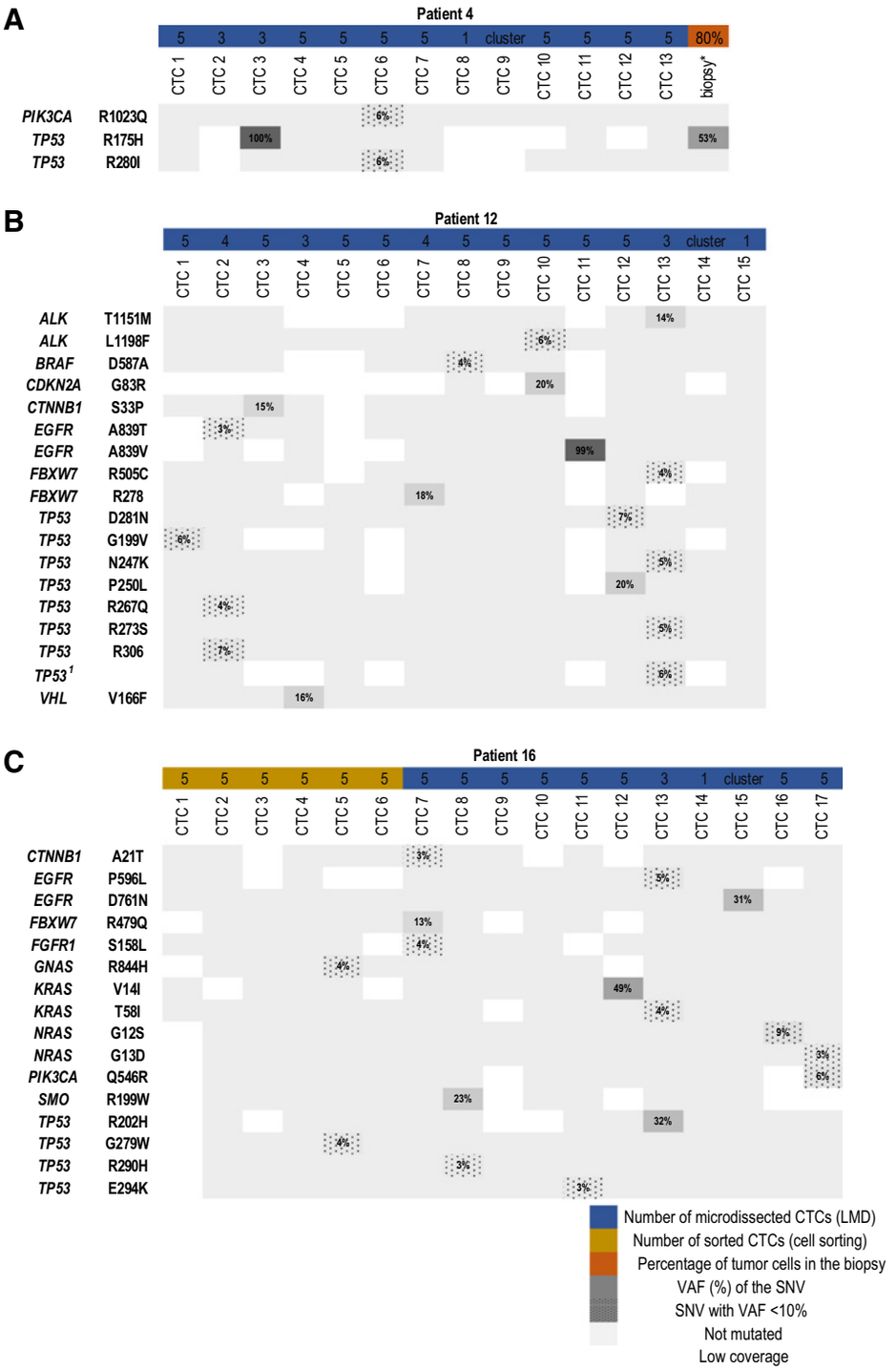

Figure 1.
Mutational profile of CTCs from *ALK*-rearranged patients resistant to crizotinib. All samples underwent targeted NGS using the two panels. Examples of P4 who developed primary resistance (**A**) and P12 (**B**) and P16 (**C**) with acquired resistance. The mutational profile of the matched tumor biopsy of P4 is presented. Tumor biopsies were not available for P12 and P16. Individual CTCs isolated by LMD from ISET filters were either grouped in pools of three to five CTCs of similar phenotype prior to the molecular analysis or analyzed as true single cells or CTC clusters. A CTC cluster is composed of more than four CTCs as previously described (31). In P16, pools of five CTCs were isolated by FACS.

(VAFs, 6%) were detected in CTC-6 specimen of this patient. P12 harbored the ALK^{T1151M} and ALK^{L1198F} mutations in different CTC specimens (VAFs, 14% and 6% respectively). In addition, this patient harbored a total of 16 "off-target" mutations (VAF ranging from 3% to 99%) in different CTC specimens including an $EGFR^{A839V}$ mutation (VAF, 99%). P13 harbored an ALK^{L1196M} mutation in the tumor biopsy that was not detected in CTCs, whereas a total of 19 "off-target" mutations including eight *TP53* mutations were detected in the 14 CTC specimens of this patient (VAF range, 3%–32%). P16 presented $EGFR^{D761N}$ and $KRAS^{V14I}$ mutations in different CTC specimens (VAF, 31% and 49% respectively) and additional 14 "off-target" mutations (VAF range, 3%–32%), all in distinct CTC specimens. The ALK^{R1275Q} mutation (VAF, 8%)

described as activating in patients with neuroblastoma was found in a CTC specimen of P32 but not in the tumor biopsy, as well as nine "off-target" mutations including *TP53* (VAF range, 3%–25%; ref. 50). Variable numbers of "off-target" mutations were detected in CTC specimens from P14, P23, P43, and P49 (VAF range, 3%–38%). Eight of the nine patients harbored *TP53* mutations in CTC specimens with variable VAF. Thus, cooccurring mutations in various ALK-independent pathways were predominantly identified in CTC specimens of crizotinib-resistant patients with *TP53* mutations being the most frequent. Importantly, these mutations were in the vast majority of cases detected in only one CTC specimen. We then asked whether some genes were recurrently mutated across patients and mapped their mutational landscape in ALK-independent signaling pathways (Fig. 2). The RTK-KRAS pathway gathered the highest number of mutated genes with a total of nine mutated genes across CTC specimens from the 9 patients. *EGFR*, *KRAS*, and *BRAF* were the most frequently mutated genes with frequency of 14.1%, 7.8%, and 6.2% respectively across mutated CTC specimens. Five of the nine patients harbored *EGFR* mutations in their CTCs. Four patients harbored *KRAS* mutations and 3 patients *BRAF* mutations. The TP53 pathway including mainly the *TP53* gene was recurrently mutated in about half of CTC specimens. HIF and NOTCH pathways were each mutated in about 9% of mutated CTC specimens and in five of nine patients for both pathways. Overall, these data show a genomic heterogeneity of an unexpected extend in CTCs from *ALK*-rearranged patients resistant to crizotinib with a variety of cooccurring mutations in genes in ALK-independent pathways, the RTK-KRAS and TP53 pathways being predominant.

Detection of mutations in CTCs from lorlatinib-resistant patients

Mutations were examined in CTCs from three patients (P41, P45, and P48) resistant to lorlatinib. In contrast to crizotinib-resistant patients, "off-target" mutations were not detected in CTCs from these patients (data not shown). *ALK* resistance mutations were only detected in P45. As shown in Fig. 3A, P45 received crizotinib, ceritinib, and brigatinib for 9.5, 1.5, and 3 months respectively prior to lorlatinib for 4 months. At PD on lorlatinib, the patient underwent a tumor biopsy and was sampled for CTC analysis. ALK^{G1202R} and ALK^{F1174L} were detected with a VAF of 29% and 9% respectively in the tumor biopsy (Fig. 3C). Sequence analysis indicated that the two mutations were present on the same allele (data not shown; ref. 51). By the CellSearch, two CTCs were enumerated in P45, a result which is consistent with the low counts of CTCs commonly detected by this technique in NSCLC patients (Supplementary Table S2). Using the second isolation strategy combining RosetteSep-enrichment and FACS, 12 single CTCs were isolated (Fig. 3B; Supplementary Table S2). *ALK* resistance mutations were identified in two single CTCs. CTC-1 harbored $ALK^{G1202R/F1174C}$ compound mutations with a VAF of 32% and 31% respectively as shown by sequence analysis (Fig. 3C; Supplementary Fig. S5A). CTC-10 harbored $ALK^{G1202R/T1151M}$ compound mutation with a VAF of 98% and 100% respectively (Fig. 3C; Supplementary Fig. S5B). Notably, the $ALK^{G1202R/T1151M}$ compound mutation was not detected in the tumor biopsy. The high frequency of $ALK^{G1202R/T1151M}$ compound mutation could be explained by the loss of *ALK*-native allele. Given the small number of SNPs that can be detected on chromosome 2 with our targeted panels, available data did not allow to strictly demonstrate this hypothesis (data

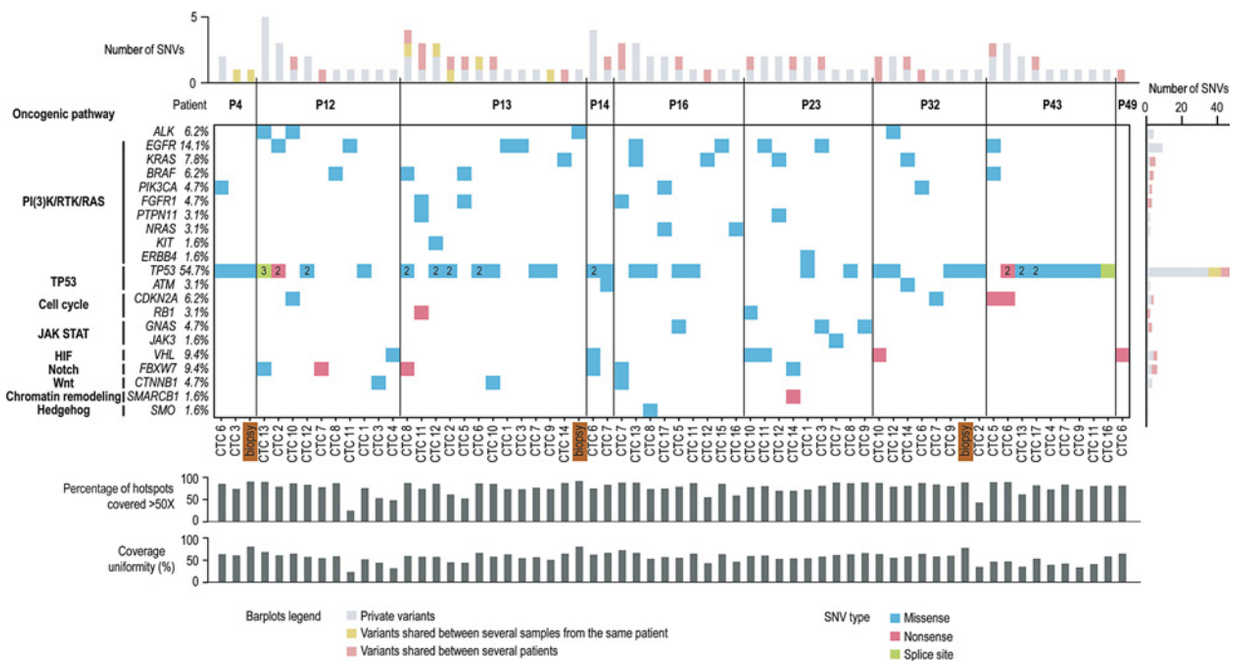

Figure 2.

Genetic landscape of CTCs and matched tumor biopsies from *ALK*-positive patients resistant to crizotinib. All samples underwent targeted NGS using the two panels.

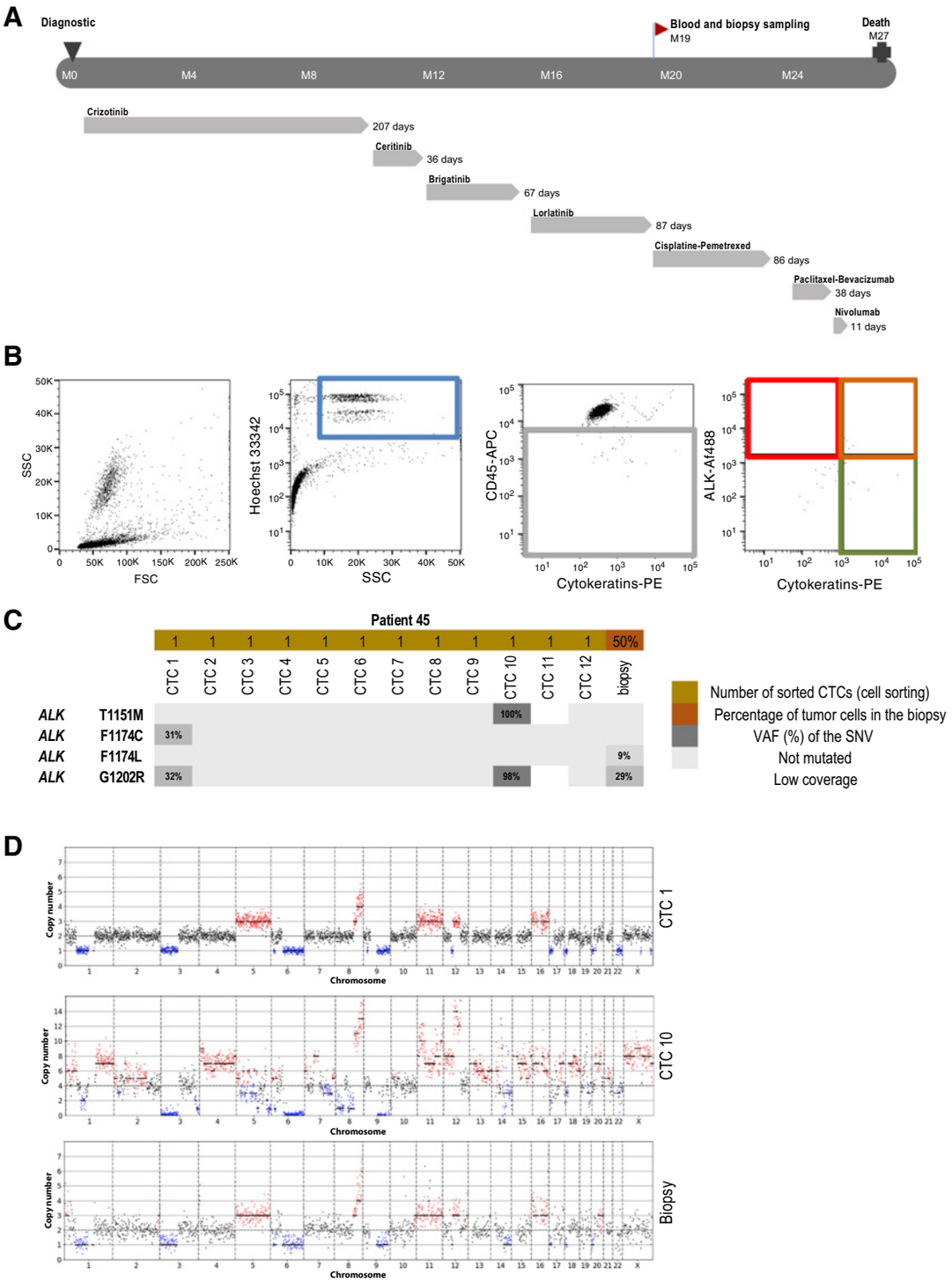

Figure 3.

Detection of *ALK* resistance compound mutations in single CTCs of a lorlatinib-resistant patient. **A,** The treatment course of P45. The patient received three lines of ALK inhibitor therapy before lorlatinib. The point at which the patient underwent blood sampling for CTC analysis and tumor biopsy is indicated. **B,** Isolation of single CTCs by FACS. **C,** Detection of *ALK* compound mutations in two single CTCs among 12 and the matched tumor biopsy of P45. All samples underwent targeted NGS using the two panels. **D,** Chromosomal CNA profiles from P45 tumor biopsy and single CTCs which harbored *ALK* resistance compound mutations using Ampli1 Low Pass sequencing.

not shown). LOH is usually observed in chromosomally unstable cancer cells. The analysis of CNA in CTC-10 indeed showed elevated copy-number heterogeneity and whole-genome duplication (WGD; Fig. 3D; Supplementary Fig. S6). WGD was not observed in either CTC-1 or the tumor biopsy (Fig. 3D). Overall, these data showed a high degree of mutational heterogeneity in CTCs from P45 with only two CTCs out of 12 harboring distinct *ALK* resistance compound mutations.

Discussion

We present the first study of mutational profiling of CTCs to identify resistance mechanisms to ALK-TKI in *ALK*-rearranged NSCLC patients. "Off-target" resistance mechanisms may be predominant on progression on crizotinib. Here, we identified an array of cooccurring mutations in ALK-independent pathways in 9 of the 14 crizotinib-resistant patients, the RTK-KRAS pathway including *EGFR*, *KRAS*, and *BRAF* genes and the TP53 pathway being predominantly mutated across patient CTCs, a result consistent with ctDNA analysis (52). Overall, our data reveal a genomic heterogeneity of an unexpected extend in CTCs from *ALK*-rearranged patients resistant to crizotinib with a variety of cooccurring mutations in different genes in ALK-independent pathways, and this information is critical to direct therapeutic choices. Furthermore, in one lorlatinib-resistant patient, we identified two compound *ALK* mutations, an "on-target" resistance mechanism recently described in *in vitro* models, and patient biopsies (17, 18).

The liquid biopsy is noninvasive, easily accessible, repeatable, and may offer a huge benefit for tracking genetic events that are causing resistance. Sequencing CTCs at the single-cell level can provide a comprehensive representation of tumor genomic heterogeneity and resistant cell clones, but it is technically challenging and requires robust workflows for individual CTC isolation, molecular analysis, and bioinformatic processing. It is noteworthy that there is no universal method allowing to capture the morphologic and phenotypical heterogeneity of CTCs (27). Based on our previous studies showing the superiority of ISET-enrichment for high cell recovery in *ALK*-FISH experiments, we initially used filtration in conjunction to LMD to isolate individual CTCs in crizotinib-resistant patients (29, 31, 32). This first strategy proved to be technically delicate, time-consuming, and difficult to use for single CTC isolation in a clinical setting. This led us to develop two supplementary strategies, and in particular hematopoietic blood-cell depletion and individual CTC sorting by FACS which proved to be simpler and more effective for isolating individual CTCs. Given the limited volume of blood samples, it was not possible to compare these different approaches in the same patients which may be considered as a limitation of our study. Once isolated at the single-cell level, CTCs must undergo WGA—a mandatory process to identify CTC somatic variants but prone to amplification bias, polymerase errors, and ADO. Several teams including our own have validated the performance of Ampli1 WGA kit combined to NGS for single CTC profiling (38, 48, 53). A global workflow was established including rigorous qualification of WGA uniformity and NGS data as well as a robust bioinformatic process allowing to distinguish artifactual variants created by the WGA from real mutations present in individual CTCs. Rigorous bioinformatic filters were applied that could also have resulted in the loss of true somatic variants. Clinically relevant mutations can be missed or lost due to the CTC isolation processes or molecular workflow, and this can be the case of P13 for whom the ALK^{L1196M} mutation found in the tumor biopsy was not detected in CTCs. Alternatively, we detected mutations in CTCs that were not detected in the matched single-site tumor biopsy, including the ALK^{R1275Q} and numerous "off-target" mutations. This suggests that CTCs harboring these mutations might derive from distinct metastatic sites or represented minor subclones that were undetectable in tumor biopsies.

Furthermore, our study is limited to a single time point (i.e., disease progression) and does not allow us to monitor a longitudinal change in the mutational profile during treatment that correlates to the clinical presentation of resistance. In spite of these limitations, our analysis of CTCs at the single-cell level revealed highly heterogeneous mutational profiles in both ALK-independent and ALK-dependent pathways and a genetic diversity of CTCs that can be clinically informative.

Studies conducted in different cohorts of *ALK*-rearranged patients have identified somatic mutations in *EGFR*, *KRAS*, *RIT1*, *MET*, *PI3KCA*, *NF1*, *NF2*, and *TP53* genes as bypass resistance mechanisms in post-crizotinib biopsies (6, 12, 14, 15, 19). By sequencing CTCs at the single-cell level, we detected a large array of mutated genes ($n = 20$) and cooccurring mutations in nine different bypass oncogenic pathways. The RTK-KRAS and TP53 pathways already identified by others were found predominant, whereas mutated pathways such as cell cycle or JAK/STAT were not previously reported. This result suggests that CTCs are prone to represent a large variety and genetic heterogeneity resistance mechanisms to ALK inhibitors, possibly in reason of their distinct spatial metastatic origins. Strikingly these mutations were in the vast majority of cases detected in only one CTC sample, a result which underlines the great genomic heterogeneity of CTCs. However, this analysis did not allow assessing the nature of the mutations (i.e., driver or passenger) and whether it is clinically relevant. Interestingly, we observed that P12 harbored both $CDKN2A^{G83R}$ and ALK^{L1198F} mutations; this was later described to be sensitive to crizotinib (54). Despite the presence of the ALK^{L1198F} mutation, resistance to crizotinib may potentially develop through a bypass mechanism involving *CDKN2A* know to regulate cell-cycle pathways or through a nontested gene. We found that the TP53 pathway was recurrently mutated in about half of CTC specimens. This is in agreement with the study conducted by Yu and colleagues who recently reported that *TP53* is frequently mutated in post-crizotinib biopsies and correlates with poor PFS in crizotinib-resistant patients (15). Overall, our results show that multiple bypass signaling pathways are highly mutated in CTCs from crizotinib-resistant patients. This corroborates with recent results obtained from post-crizotinib biopsies showing the importance of bypass signaling pathway mechanisms in crizotinib and ALK-TKI resistance (14). This also suggests that CTC sequencing may be a helpful tool to track resistance mutations in bypass pathways, inform drug resistance mechanism, and contribute to develop new therapeutic strategies.

ALK resistance mutations were detected in two single CTCs of P45 who was sequentially treated by four ALK inhibitors including lorlatinib. The first single CTC harbored the $ALK^{G1202R/F1174C}$ compound mutation, whereas the $ALK^{G1202R/F1174L}$ compound mutation was detected in the tumor biopsy obtained at the time of CTC sampling. The G1202, which maps to the solvent-exposed region of ALK protein, and the F1174 adjacent to the C-terminus of the αC helix are common mutated positions described in *ALK*-rearranged patients. The C/L amino acid difference between CTCs and the tumor biopsy may represent an additional level of

mutational heterogeneity in P45. A multitude of single *ALK* kinase domain mutations can emerge on first and second lines of ALK-TKI and are the substrates for diverse compound mutations (17, 18). Among these, compound mutants containing the ALK^{G1202R} are predicted to be highly refractory to ALK inhibitors based on structural studies. These studies suggested that ALK^{G1202R} can destabilize lorlatinib binding due to steric and conformational effects induced by the arginine substitution, whereas $ALK^{F1174C/L}$ can contribute to increase the ATP-binding affinity of ALK (18). Combination of ALK^{G1202R} and $ALK^{F1174C/L}$ is expected to significantly impede the efficacy of lorlatinib and favor the emergence of a resistant mutant clone. The most striking finding was the detection of a different and unpublished compound mutation (i.e., $ALK^{G1202R/T1151M}$) at a high frequency in a second single CTC that was not detected in the tumor biopsy. This CTC may represent a resistant cell clone that derived from a metastatic site or was undetectable in the single-tumor biopsy as mentioned above. This CTC presented a high degree of chromosomal instability and WGD which could have caused loss of *ALK*-native allele. WGD may precede subclonal diversification of CNAs and subsequent large-scale single-copy losses and has been associated with poor prognosis across cancer types (55). By generating important genetic diversity, this phenomenon may provide cells with the necessary adaptations to survive blood transit and seed metastases. Overall, data from P45 suggest that genomic analysis of single CTCs can be an effective mean of tracking gene alterations present in minor resistant cancer clones that are not detected in bulk tumor samples or single-site biopsies. These data also highlight the high degree of mutational heterogeneity of CTCs as well as certain genomic features that can provide information on new drug resistance mechanisms.

Altogether, our results show that mutational profiling of CTCs can provide unique insight into the heterogeneous mechanisms of resistance to ALK-TKI that is otherwise inaccessible. These findings emphasize the potential clinical utility of single CTC sequencing to identify circulating resistant cell clones that are arguably an important subset of cancer cells to target and eradicate. By offering real-time monitoring of a constantly evolving disease and by detecting crucial mutations through simple blood draws, CTCs' sequencing may be of great utility to help clinicians to personalize treatment at progression. Further validation and qualification studies are needed within international consortia such as the EU/IMI CANCER-ID consortium for the future implementation of CTC assays into clinical practice. Finally, the clinical relevance of heterogeneity is yet to be defined by demonstrating how it can guide therapy and affect patient outcomes.

Disclosure of Potential Conflicts of Interest

L. Mezquita reports receiving speakers bureau honoraria from Bristol-Myers Squibb and Tecnofarma, and is a consultant/advisory board member for Roche. D. Planchard is an employee of and has ownership interests (including patents) at AstraZeneca, Bristol-Myers Squibb, Celgene, Eli Lilly, Merck, Novartis, Pfizer, priME Oncology, Peer CME, Roche and Boehringer Ingelhim, and is a consultant/advisory board member for MedImmune. B. Besse reports receiving commercial research support from Abbvie, Amgen, AstraZeneca, Blueprint Medicine, Bristol-Myers Squibb, Boehringer Ingelheim, Celgene, Cristal Therapeutics, Eli Lilly, GlaxoSmithKline, Ignyta, IPSEN, Janssen, Merck KGaA, MSD, Nektar, Onxeo, OSE Immunopharmaceuticals, Pfizer, Pharma Mar, Sanofi, Spectrum Pharmaceuticals, Takeda, and Tiziana Pharma. No potential conflicts of interest were disclosed by the other authors.

Authors' Contributions

Conception and design: E. Pailler, V. Faugeroux, D. Planchard, B. Besse, F. Farace

Development of methodology: E. Pailler, V. Faugeroux, M. Oulhen, L. Mezquita, L. Lacroix, F. Farace

Acquisition of data (provided animals, acquired and managed patients, provided facilities, etc.): E. Pailler, V. Faugeroux, M. Oulhen, L. Mezquita, Y. Lecluse, P. Queffelec, M. NgoCamus, C. Nicotra, J. Remon, L. Lacroix, D. Planchard, L. Friboulet, B. Besse

Analysis and interpretation of data (e.g., statistical analysis, biostatistics, computational analysis): E. Pailler, V. Faugeroux, M. Oulhen, L. Mezquita, D. Planchard, B. Besse, F. Farace

Writing, review, and/or revision of the manuscript: E. Pailler, V. Faugeroux, L. Mezquita, L. Lacroix, D. Planchard, B. Besse, F. Farace

Administrative, technical, or material support (i.e., reporting or organizing data, constructing databases): E. Pailler, V. Faugeroux, M. Oulhen, L. Mezquita, M. Laporte, A. Honoré, Y. Lecluse, P. Queffelec, C. Nicotra, J. Remon

Study supervision: E. Pailler, F. Farace

Acknowledgments

The authors are grateful to the patients and their families. The authors thank Dr. Philippe Vielh and Professor Jean-Yves Scoazec for critical insights and discussions, Virginie Marty for expert technical assistance, and Laëtitia Millier for very effective secretary assistance. They also thank Menarini Silicon Biosystems particularly Nicolò Manaresi to provide us the Ampli1 Cancer Hotspot Panel Custom Beta, and Genny Buson, Marianna Garonzi, and Claudio Forcato for the help in generating and analyzing the Ampli1 LowPass data. They thank Integragen for help in NGS bioinformatic analysis, Leica Biosystems for the development of the ALTER software, and Thermo Fisher Scientific for the development of primer panels.

E. Pailler was supported by the LabEx LERMIT (grant no. ANR-10-LABX-0033-LERMIT) and the Fondation pour la Recherche Médicale (grant no. FDT20150532072). She received the AACR-Takeda Oncology Scholar-in-training Award for this work. V. Faugeroux was supported by the Fondation pour la Recherche Médicale (grant no. FDT20160435543). This work was also supported by the Institut National du Cancer (PRT-K14-032), the Agence Nationale de la Recherche (ANR-CE17-0006-01), the Fondation de France (grant no. 201300038317), the Fondation ARC pour la Recherche sur le Cancer (grant no. 20131200417), and the Innovative Medicines Joint Undertaking CANCER ID (IMI-JU-11-2013, grant no. 115749).

The costs of publication of this article were defrayed in part by the payment of page charges. This article must therefore be hereby marked *advertisement* in accordance with 18 U.S.C. Section 1734 solely to indicate this fact.

Received April 9, 2019; revised July 4, 2019; accepted August 13, 2019; published first August 22, 2019.

References

1. Camidge DR, Bang YJ, Kwak EL, Iafrate AJ, Varella-Garcia M, Fox SB, et al. Activity and safety of crizotinib in patients with ALK-positive non-small-cell lung cancer: updated results from a phase 1 study. Lancet Oncol 2012; 13:1011–9.
2. Shaw AT, Kim DW, Nakagawa K, Seto T, Crino L, Ahn MJ, et al. Crizotinib versus chemotherapy in advanced ALK-positive lung cancer. N Engl J Med 2013;368:2385–94.
3. Blackhall F, Ross Camidge D, Shaw AT, Soria JC, Solomon BJ, Mok T, et al. Final results of the large-scale multinational trial PROFILE 1005: efficacy and safety of crizotinib in previously treated patients with advanced/metastatic ALK-positive non-small-cell lung cancer. ESMO Open 2017; 2:e000219.
4. Shaw AT, Kim DW, Mehra R, Tan DS, Felip E, Chow LQ, et al. Ceritinib in ALK-rearranged non-small-cell lung cancer. N Engl J Med 2014;370:1189–97.

5. Ou SH, Ahn JS, De Petris L, Govindan R, Yang JC, Hughes B, et al. Alectinib in crizotinib-refractory ALK-rearranged non-small-cell lung cancer: a phase II global study. J Clin Oncol 2016;34:661–8.
6. Rotow J, Bivona TG. Understanding and targeting resistance mechanisms in NSCLC. Nat Rev Cancer 2017;17:637–58.
7. Kim DW, Tiseo M, Ahn MJ, Reckamp KL, Hansen KH, Kim SW, et al. Brigatinib in patients with crizotinib-refractory anaplastic lymphoma kinase-positive non-small-cell lung cancer: a randomized, multicenter phase II trial. J Clin Oncol 2017;35:2490–8.
8. Facchinetti F, Tiseo M, Di Maio M, Graziano P, Bria E, Rossi G, et al. Tackling ALK in non-small cell lung cancer: the role of novel inhibitors. Transl Lung Cancer Res 2016;5:301–21.
9. Horn L, Infante JR, Reckamp KL, Blumenschein GR, Leal TA, Waqar SN, et al. Ensartinib (X-396) in ALK-positive non-small cell lung cancer: results from a first-in-human phase I/II, multicenter study. Clin Cancer Res 2018; 24:2771–9.
10. Solomon BJ, Besse B, Bauer TM, Felip E, Soo RA, Camidge DR, et al. Lorlatinib in patients with ALK-positive non-small-cell lung cancer: results from a global phase 2 study. Lancet Oncol 2018;19:1654–67.
11. Camidge DR, Pao W, Sequist LV. Acquired resistance to TKIs in solid tumours: learning from lung cancer. Nat Rev Clin Oncol 2014;11:473–81.
12. Doebele RC, Pilling AB, Aisner DL, Kutateladze TG, Le AT, Weickhardt AJ, et al. Mechanisms of resistance to crizotinib in patients with ALK gene rearranged non-small cell lung cancer. Clin Cancer Res 2012;18:1472–82.
13. Gainor JF, Dardaei L, Yoda S, Friboulet L, Leshchiner I, Katayama R, et al. Molecular mechanisms of resistance to first- and second-generation ALK inhibitors in ALK-rearranged lung cancer. Cancer Discov 2016;6:1118–33.
14. McCoach CE, Le AT, Gowan K, Jones K, Schubert L, Doak A, et al. Resistance mechanisms to targeted therapies in ROS1(+) and ALK(+) non-small cell lung cancer. Clin Cancer Res 2018;24:3334–47.
15. Yu Y, Ou Q, Wu X, Bao H, Ding Y, Shao YW, et al. Concomitant resistance mechanisms to multiple tyrosine kinase inhibitors in ALK-positive non-small cell lung cancer. Lung Cancer 2019;127:19–24.
16. Katayama R, Shaw AT, Khan TM, Mino-Kenudson M, Solomon BJ, Halmos B, et al. Mechanisms of acquired crizotinib resistance in ALK-rearranged lung Cancers. Sci Transl Med 2012;4:120ra17.
17. Okada K, Araki M, Sakashita T, Ma B, Kanada R, Yanagitani N, et al. Prediction of ALK mutations mediating ALK-TKIs resistance and drug repurposing to overcome the resistance. EBioMedicine 2019;41:105–19.
18. Yoda S, Lin JJ, Lawrence MS, Burke BJ, Friboulet L, Langenbucher A, et al. Sequential ALK inhibitors can select for lorlatinib-resistant compound ALK mutations in ALK-positive lung cancer. Cancer Discov 2018; 8:714–29.
19. Recondo G, Facchinetti F, Olaussen KA, Besse B, Friboulet L. Making the first move in EGFR-driven or ALK-driven NSCLC: first-generation or next-generation TKI? Nat Rev Clin Oncol 2018;15:694–708.
20. Cai W, Lin D, Wu C, Li X, Zhao C, Zheng L, et al. Intratumoral heterogeneity of ALK-rearranged and ALK/EGFR coaltered lung adenocarcinoma. J Clin Oncol 2015;33:3701–9.
21. Jamal-Hanjani M, Wilson GA, McGranahan N, Birkbak NJ, Watkins TBK, Veeriah S, et al. Tracking the evolution of non-small-cell lung cancer. N Engl J Med 2017;376:2109–21.
22. Heitzer E, Haque IS, Roberts CES, Speicher MR. Current and future perspectives of liquid biopsies in genomics-driven oncology. Nat Rev Genet 2019;20:71–88.
23. Siravegna G, Marsoni S, Siena S, Bardelli A. Integrating liquid biopsies into the management of cancer. Nat Rev Clin Oncol 2017;14:531–48.
24. Wan JCM, Massie C, Garcia-Corbacho J, Mouliere F, Brenton JD, Caldas C, et al. Liquid biopsies come of age: towards implementation of circulating tumour DNA. Nat Rev Cancer 2017;17:223–38.
25. McCoach CE, Blakely CM, Banks KC, Levy B, Chue BM, Raymond VM, et al. Clinical utility of cell-free DNA for the detection of ALK fusions and genomic mechanisms of ALK inhibitor resistance in non-small cell lung cancer. Clin Cancer Res 2018;24:2758–70.
26. Dagogo-Jack I, Brannon AR, Ferris LA, Campbell CD, Lin JJ, Schultz KR, et al. Tracking the evolution of resistance to ALK tyrosine kinase inhibitors through longitudinal analysis of circulating tumor DNA. JCO Precis Oncol 2018;2018.
27. Alix-Panabieres C, Pantel K. Challenges in circulating tumour cell research. Nat Rev Cancer 2014;14:623–31.
28. Krebs MG, Metcalf RL, Carter L, Brady G, Blackhall FH, Dive C. Molecular analysis of circulating tumour cells-biology and biomarkers. Nat Rev Clin Oncol 2014;11:129–44.
29. Pailler E, Adam J, Barthelemy A, Oulhen M, Auger N, Valent A, et al. Detection of circulating tumor cells harboring a unique ALK rearrangement in ALK-positive non-small-cell lung cancer. J Clin Oncol 2013;31: 2273–81.
30. Pailler E, Auger N, Lindsay CR, Vielh P, Islas-Morris-Hernandez A, Borget I, et al. High level of chromosomal instability in circulating tumor cells of ROS1-rearranged non-small-cell lung cancer. Ann Oncol 2015;26: 1408–15.
31. Pailler E, Oulhen M, Billiot F, Galland A, Auger N, Faugeroux V, et al. Method for semi-automated microscopy of filtration-enriched circulating tumor cells. BMC Cancer 2016;16:477.
32. Pailler E, Oulhen M, Borget I, Remon J, Ross K, Auger N, et al. Circulating tumor cells with aberrant ALK copy number predict progression-free survival during crizotinib treatment in ALK-rearranged non-small cell lung cancer patients. Cancer Res 2017;77:2222–30.
33. Berger LA, Janning M, Velthaus JL, Ben-Batalla I, Schatz S, Falk M, et al. Identification of a high-level MET amplification in CTCs and cfTNA of an ALK-positive NSCLC patient developing evasive resistance to crizotinib. J Thorac Oncol 2018;13:e243–e6.
34. Farace F, Massard C, Vimond N, Drusch F, Jacques N, Billiot F, et al. A direct comparison of CellSearch and ISET for circulating tumour-cell detection in patients with metastatic carcinomas. Br J Cancer 2011;105:847–53.
35. Vona G, Sabile A, Louha M, Sitruk V, Romana S, Schutze K, et al. Isolation by size of epithelial tumor cells: a new method for the immunomorphological and molecular characterization of circulatingtumor cells. Am J Pathol 2000;156:57–63.
36. Allard WJ, Matera J, Miller MC, Repollet M, Connelly MC, Rao C, et al. Tumor cells circulate in the peripheral blood of all major carcinomas but not in healthy subjects or patients with nonmalignant diseases. Clin Cancer Res 2004;10:6897–904.
37. Ferrarini A, Forcato C, Buson G, Tononi P, Del Monaco V, Terracciano M, et al. A streamlined workflow for single-cells genome-wide copy-number profiling by low-pass sequencing of LM-PCR whole-genome amplification products. PLoS One 2018;13:e0193689.
38. Polzer B, Medoro G, Pasch S, Fontana F, Zorzino L, Pestka A, et al. Molecular profiling of single circulating tumor cells with diagnostic intention. EMBO Mol Med 2014;6:1371–86.
39. Martin M. Cutadapt removes adapter sequences from high-throughput sequencing reads. EMBnet Journal 2011;17.
40. Li H, Handsaker B, Wysoker A, Fennell T, Ruan J, Homer N, et al. The sequence alignment/map format and SAMtools. Bioinformatics 2009;25: 2078–9.
41. Tarasov A, Vilella AJ, Cuppen E, Nijman IJ, Prins P. Sambamba: fast processing of NGS alignment formats. Bioinformatics 2015;31:2032–4.
42. DePristo MA, Banks E, Poplin R, Garimella KV, Maguire JR, Hartl C, et al. A framework for variation discovery and genotyping using next-generation DNA sequencing data. Nat Genet 2011;43:491–8.
43. Cibulskis K, Lawrence MS, Carter SL, Sivachenko A, Jaffe D, Sougnez C, et al. Sensitive detection of somatic point mutations in impure and heterogeneous cancer samples. Nat Biotechnol 2013;31:213–9.
44. Van der Auwera GA, Carneiro MO, Hartl C, Poplin R, Del Angel G, Levy-Moonshine A, et al. From FastQ data to high confidence variant calls: the Genome Analysis Toolkit best practices pipeline. Curr Protoc Bioinformatics 2013;43:11 0 1–33.
45. McLaren W, Gil L, Hunt SE, Riat HS, Ritchie GR, Thormann A, et al. The Ensembl variant effect predictor. Genome Biol 2016;17:122.
46. Li H, Durbin R. Fast and accurate short read alignment with Burrows-Wheeler transform. Bioinformatics 2009;25:1754–60.
47. Boeva V, Popova T, Bleakley K, Chiche P, Cappo J, Schleiermacher G, et al. Control-FREEC: a tool for assessing copy number and allelic content using next-generation sequencing data. Bioinformatics 2012;28:423–5.
48. Faugeroux V, Lefebvre C, Pailler E, Pierron V, Marcaillou C, Tourlet S, et al. An accessible and unique insight into metastasis mutational content through whole-exome sequencing of circulating tumor cells in metastatic prostate cancer. Eur Urol Oncol 2019. Available from: https://www-ncbi-nlm-nih-gov.gate2.inist.fr/pubmed/31412010; https://euoncology.europeanurology.com/article/S2588-9311(18)30213-X/fulltext.

49. Ilie M, Long E, Butori C, Hofman V, Coelle C, Mauro V, et al. ALK-gene rearrangement: a comparative analysis on circulating tumour cells and tumour tissue from patients with lung adenocarcinoma. Ann Oncol 2012;23:2907–13.
50. Bresler SC, Weiser DA, Huwe PJ, Park JH, Krytska K, Ryles H, et al. ALK mutations confer differential oncogenic activation and sensitivity to ALK inhibition therapy in neuroblastoma. Cancer Cell 2014;26:682–94.
51. Recondo G, Mezquita L, Planchard D, Gazzah A, Facchinetti F, Bigot L, et al. Diverse resistance mechanisms to the third-generation ALK inhibitor lorlatinib in ALK-rearranged lung cancer. 2019. DOI: 10.1158/1078-0432.CCR-19-1176.
52. Mezquita L, Swalduz A, Jovelet C, Ortiz-Cuaran S, Planchard D, Avrillon V, et al. P1.01-67 clinical relevance of ALK/ROS1 resistance mutations and other acquired mutations detected by liquid biopsy in advanced NSCLC patients. J Thorac Oncol 2018:S487–S88.
53. Babayan A, Alawi M, Gormley M, Muller V, Wikman H, McMullin RP, et al. Comparative study of whole genome amplification and next generation sequencing performance of single cancer cells. Oncotarget 2017;8:56066–80.
54. Shaw AT, Friboulet L, Leshchiner I, Gainor JF, Bergqvist S, Brooun A, et al. Resensitization to crizotinib by the lorlatinib ALK resistance mutation L1198F. N Engl J Med 2016;374:54–61.
55. Bielski CM, Zehir A, Penson AV, Donoghue MTA, Chatila W, Armenia J, et al. Genome doubling shapes the evolution and prognosis of advanced cancers. Nat Genet 2018;50:1189–95.